10.3 Macroscopic Quantum State

Josephson effects (1962)

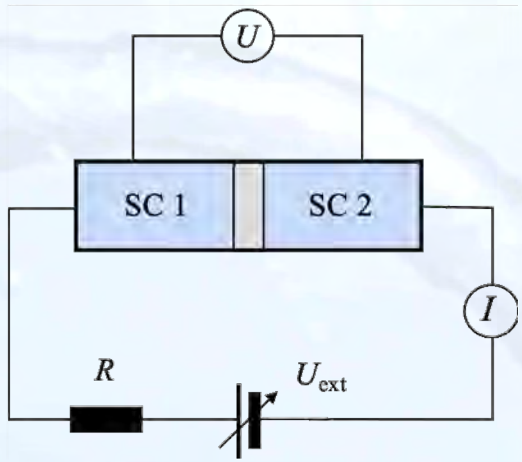

Brain Josephson

Schrödinger equations

$$\mathrm{i}\hbar\dot{\Psi}_1 = \mu_1\Psi_1 + \mathcal{K}\Psi_2$$

$$\mathrm{i}\hbar\dot{\Psi}_2 = \mu_2\Psi_2 + \mathcal{K}\Psi_1$$

chemical potential (μ_2) — coupling strength ($\mathcal{K}$)

ansatz $\Psi_1 = \sqrt{n_{s1}}\mathrm{e}^{\varphi_1}$ and $\Psi_2 = \sqrt{n_{s2}}\mathrm{e}^{\varphi_2}$

with $n_s = n_{s1} = n_{s2}$

Josephson equations

$$\dot{n}_{s1} = \frac{2\mathcal{K}}{\hbar}\, n_s \sin(\varphi_2 - \varphi_1) = -\dot{n}_{s2}$$

$$\hbar(\dot{\varphi}_2 - \dot{\varphi}_1) = -(\mu_2 - \mu_1) = 2eV$$

$V = 0 \longrightarrow \mu_1 = \mu_2 \longrightarrow I_s = I_c \sin(\varphi_2 - \varphi_1)$ dc Josephson effect

$V \neq 0 \longrightarrow \mu_2 - \mu_1 = -2eV \longrightarrow I_s = I_c \sin(\omega_J t + \varphi_0)$ ac Josephson effect

$\omega_J = 2eV/\hbar$

10.3 Macroscopic Quantum State

Experimental observation of dc Josephson effect

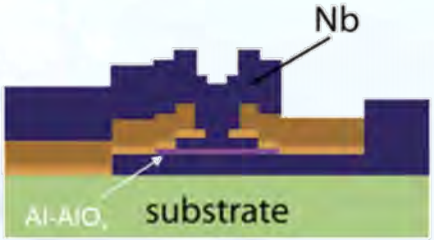

Josephson junction

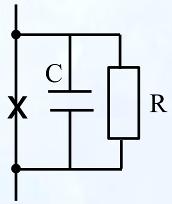

hysteresis parameter: $\beta_c = 2\pi I_c R^2 C/\Phi_0$

underdamped junction (large *R* and *C*)

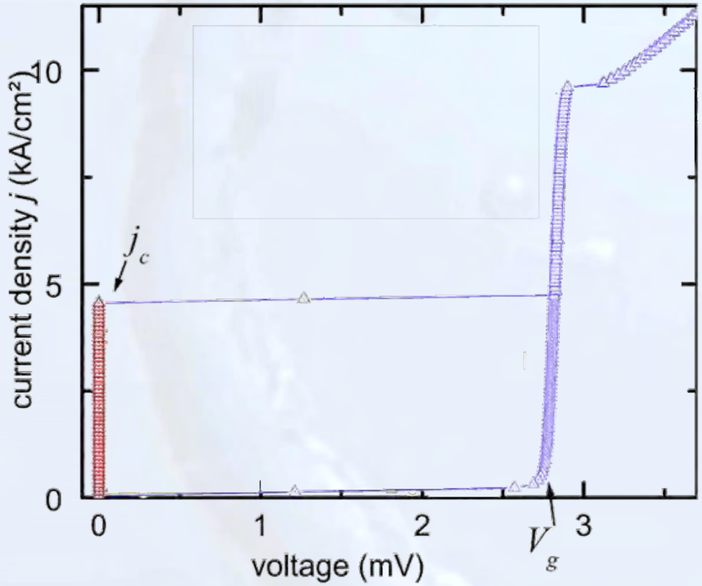

- hysteretic Josephson junction
- for $I < I_c$ current is determined by current source
- for $I > I_c$ super current breaks down

overdamped junction (small *R* and *C*)

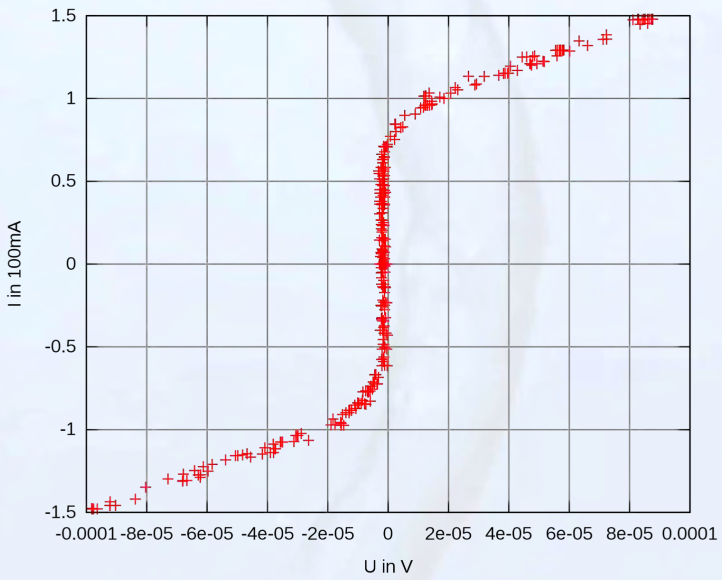

- non-hysteretic Josephson junction
- for $I > I_c$ super current breaks down

10.4 Unconventional Superconductors

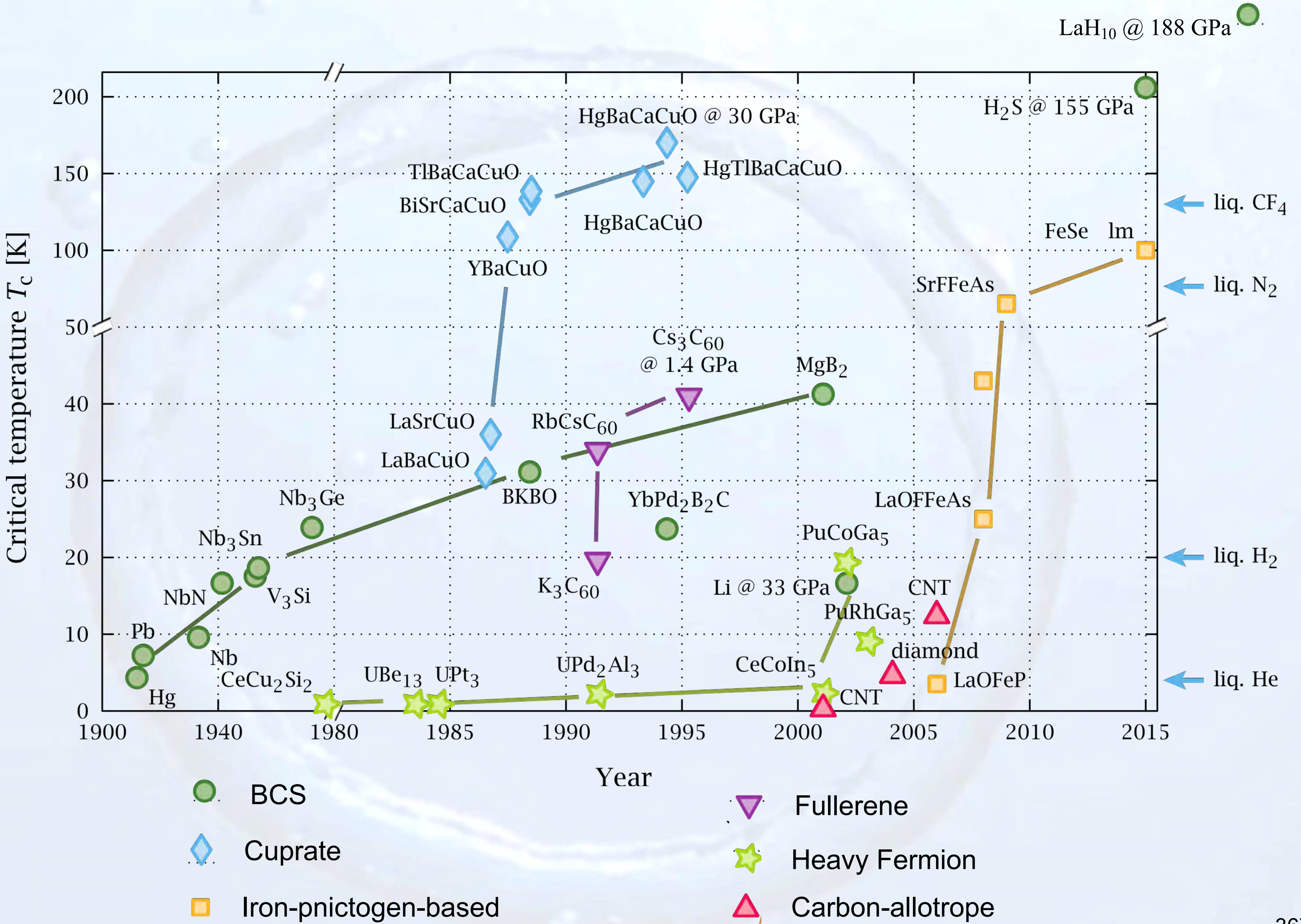

10.4 Unconventional Superconductors

Quantum states

		S	*L*
s–wave	conventional superconductors	0	0
p–wave	(Sr_2RuO_4)	1	1
d–wave	cuprate high-T_c superconductors	0	2
f–wave	(UPt_3)	1	3

energy gap $\Delta_{\boldsymbol{k}} = \Delta_0(T) f(\widehat{\boldsymbol{k}})$		nodes	$f(\widehat{\boldsymbol{k}})$
conventional superconductors	isotropic	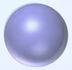	1
cuprate high-T_c superconductors	2D		$k_x^2 - k_y^2$
Sr_2RuO_4	axial 2D		$(\widehat{k}_x^2 - \widehat{k}_y^2)(\widehat{k}_x + \mathrm{i}\widehat{k}_y)$
UPt_3	3D	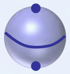	$\widehat{k}_z(\widehat{k}_x + \mathrm{i}\widehat{k}_y)^2$
UBe_{13}	axial 3D	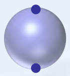	$\widehat{k}_x + \mathrm{i}\widehat{k}_y$

10.4 Unconventional Superconductors

cuprate high-T_c superconductors

discovered June 1986

Possible High T_c Superconductivity in the Ba – La – Cu – O System

J.G. Bednorz and K.A. Müller
IBM Zürich Research Laboratory, Rüschlikon, Switzerland

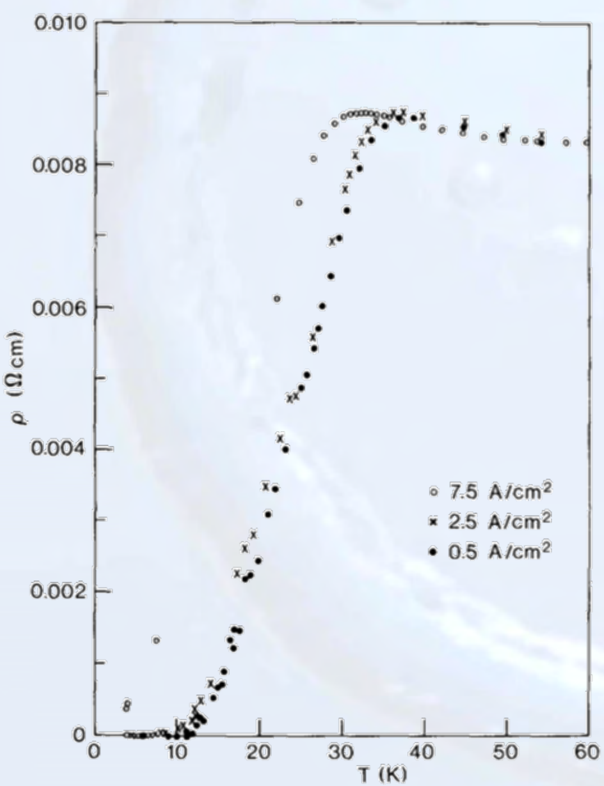

Georg Bednorz Karl Alexander Müller

APS March Meeting of 1987
The "Woodstock of Physics“ Hilton Hotel New York

10.4 Unconventional Superconductors

best investigated system: YBCO Yttrium barium copper oxide

important are the Cu-O planes ⟶ different phases depending on hole concentration introduced by oxygen surplus

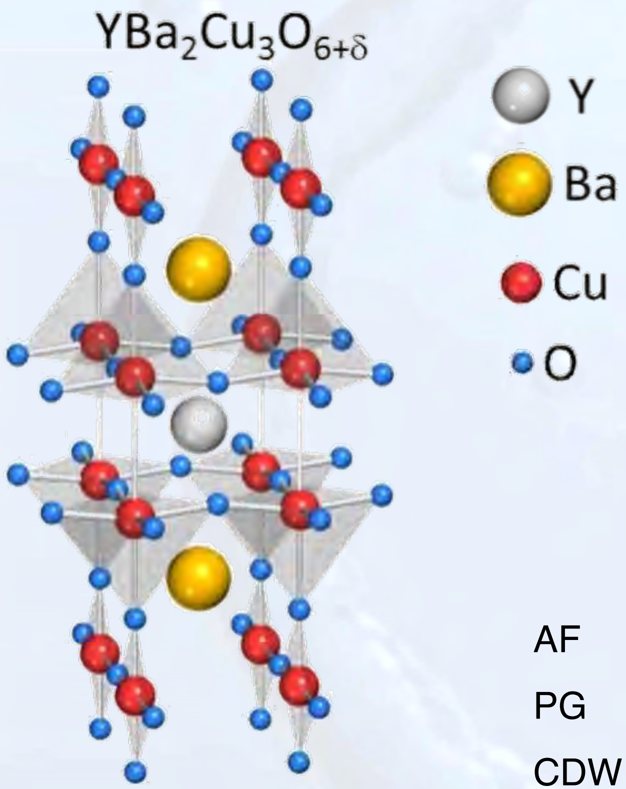

perovskite structure

$0 < \delta < 0.4$	insulator
$\delta \approx 0.4$	insulator-metal transition
$\delta > 0.4$	superconductor
$\delta = 0.92$	superconductor with T_c = 95 K

AF anti-ferromagnetic phase
PG pseudo gap
CDW charge density wave
SM strange metal
FL Fermi liquid phase

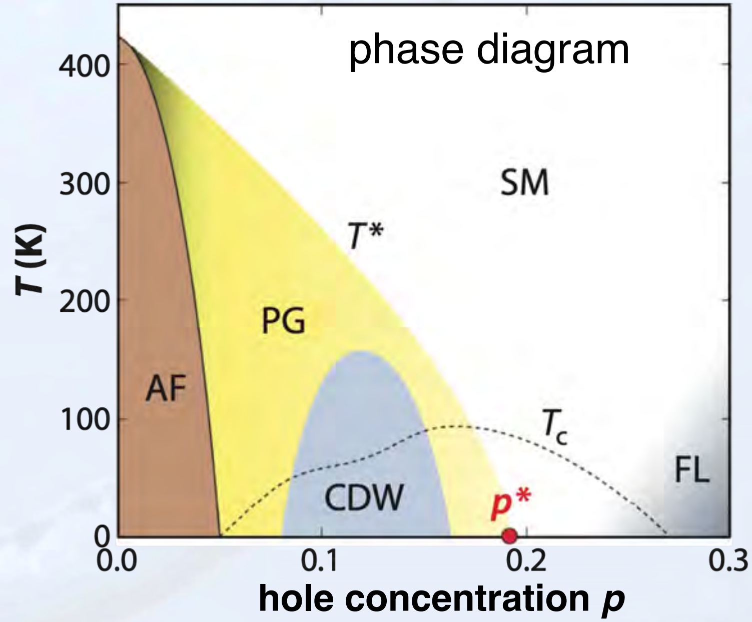

10.4 Unconventional Superconductors

superconducting transition

a) resistance

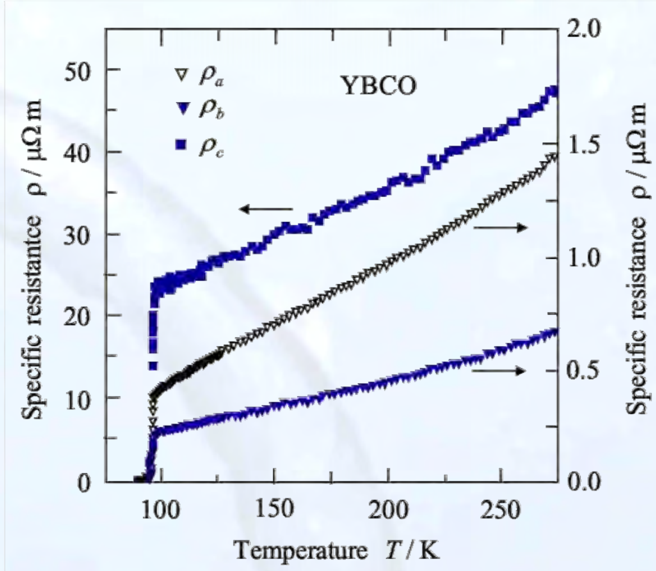

- ► resistivity depends on crystal direction
- ► in *c*-direction (perpendicular to CuO_2 planes) resistivity is much higher

b) specific heat

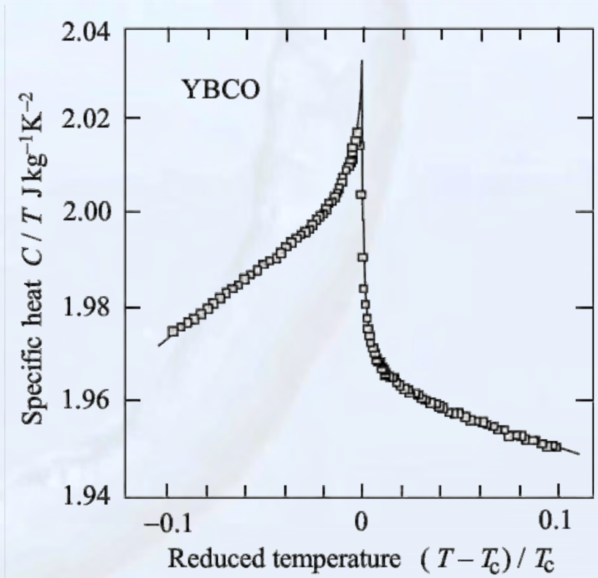

- ► second order phase transition
- ► rounded onset of transition caused by large fluctuation
  ⟶ indicates short coherence length

10.4 Unconventional Superconductors

Critical fields

$$B_{c1} = \frac{\Phi_0}{4\pi\lambda_L^2}$$

- B_{c1} depends on crystal direction
- B_{c1} is very small at $T = 0$

→ $\lambda_L = 150$ nm → factor 10 larger as for Al

→ $\lambda_L^2 \propto 1/n_s$ → factor 100 less Cooper pairs

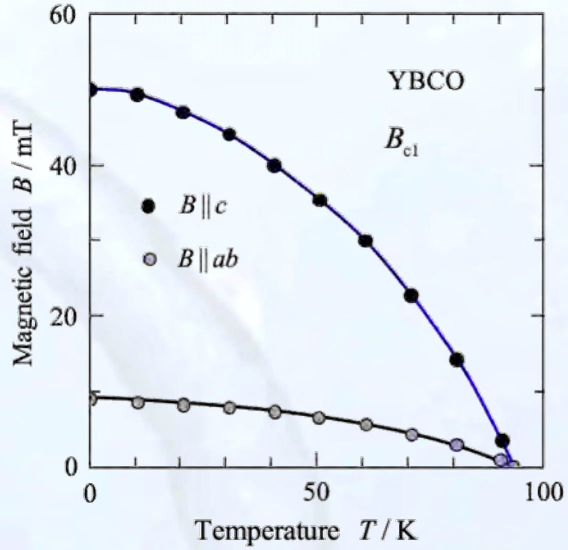

$$B_{c2} = \frac{\Phi_0}{2\pi\xi_{GL}^2}$$

- B_{c2} depends on crystal direction
- B_{c2} is very large at $T = 0$ → $B_{c2} >$ 800 T for $B \| ab$

→ very small coherence length $\xi_{GL} = 1.5$ nm

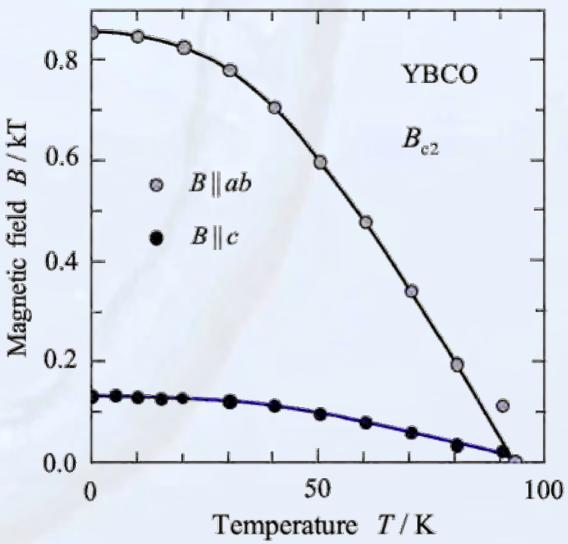

→ $\lambda_L \gg \xi_{GL}$ → extreme type II superconductor

Experimental determination of *d*-wave nature of Cooper pairs inYBCO

- flux quantization
- Josephson effect

a) flux quantization

normal geometry -- YBCO ring

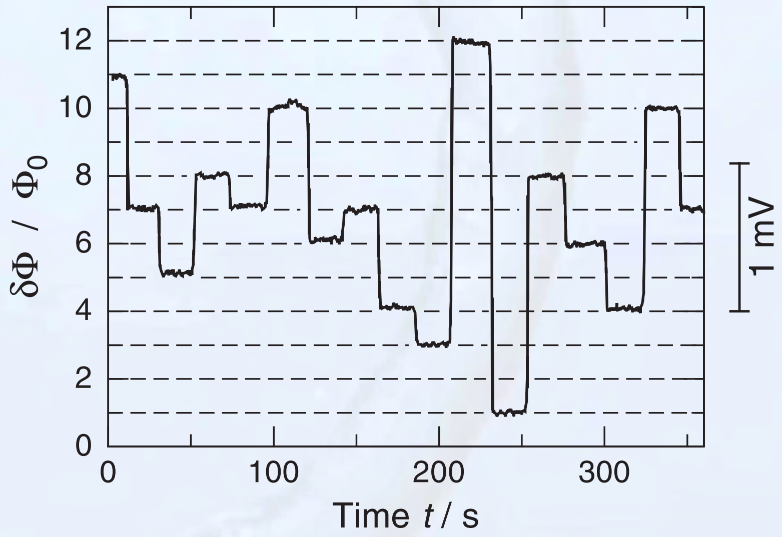

- flux quantization measured with SQUID
- result: Φ_0 = h/2e

10.4 Unconventional Superconductors

Experimental determination of *d*-wave nature of Cooper pairs in YBCO

unconventional flux quantization

tri-crystalline rings

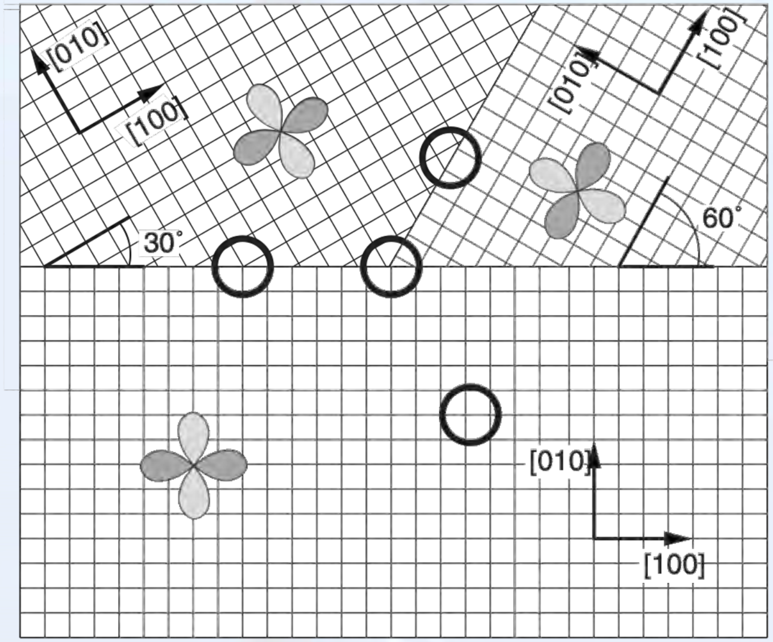

- YBCO film is grown epitaxially on $SrTiO_3$ substrate
- $SrTiO_3$ is suitably tailored having 3 crystal orientations
- YBCO is patterned by ion milling to produces rings
- rings are positioned that they contain grain boundaries
- macroscopic quantum states in different parts of the rings have different orientations
- the grain boundaries produce π junctions

↗ 0 or even number of π junctions $\Phi = n\Phi_0$

↘ odd number of π junctions $\Phi = \left(n + \frac{1}{2}\right)\Phi_0$ ⟶ half-flux quantum

10.4 Unconventional Superconductors

Experimental result

scanning SQUID microscopy

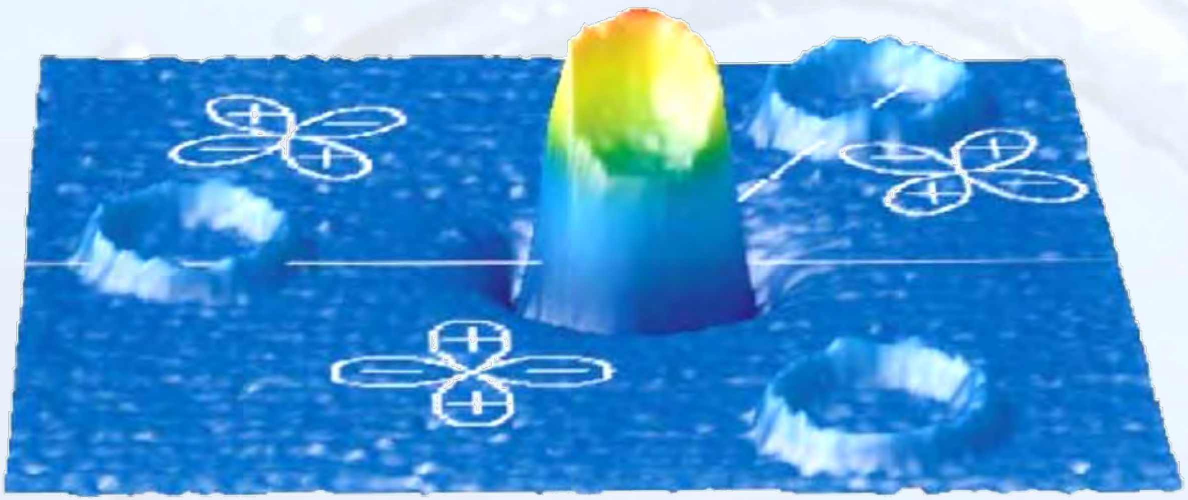

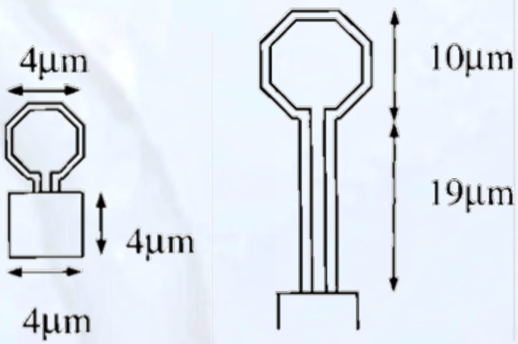

- rings with even number of π junctions show no flux
- ring in the middle with 3 π junctions shows spontaneous formation of half-flux quantum

11. Cooling Techniques

^{4}He Bath Cryostat: Glass-Dewar

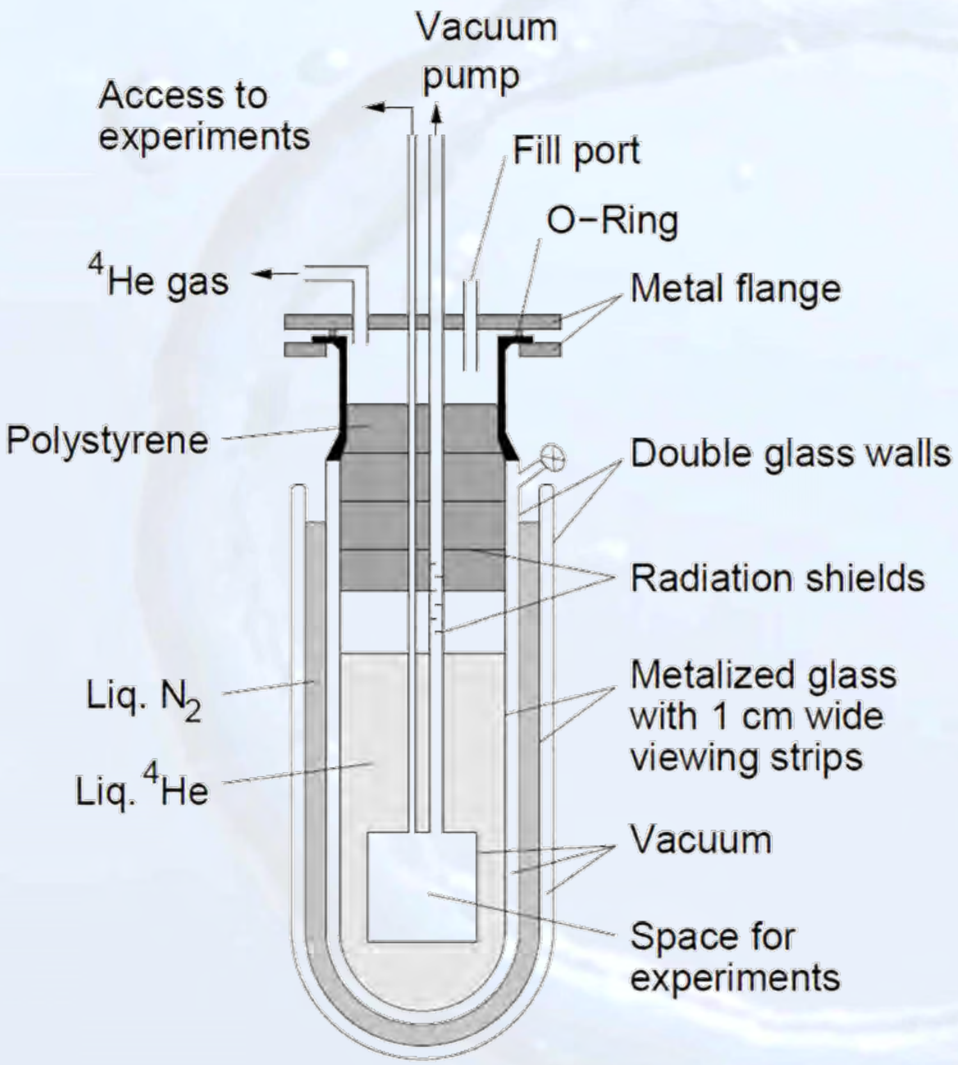

^{4}He Bath Cryostat: Metal-Dewar

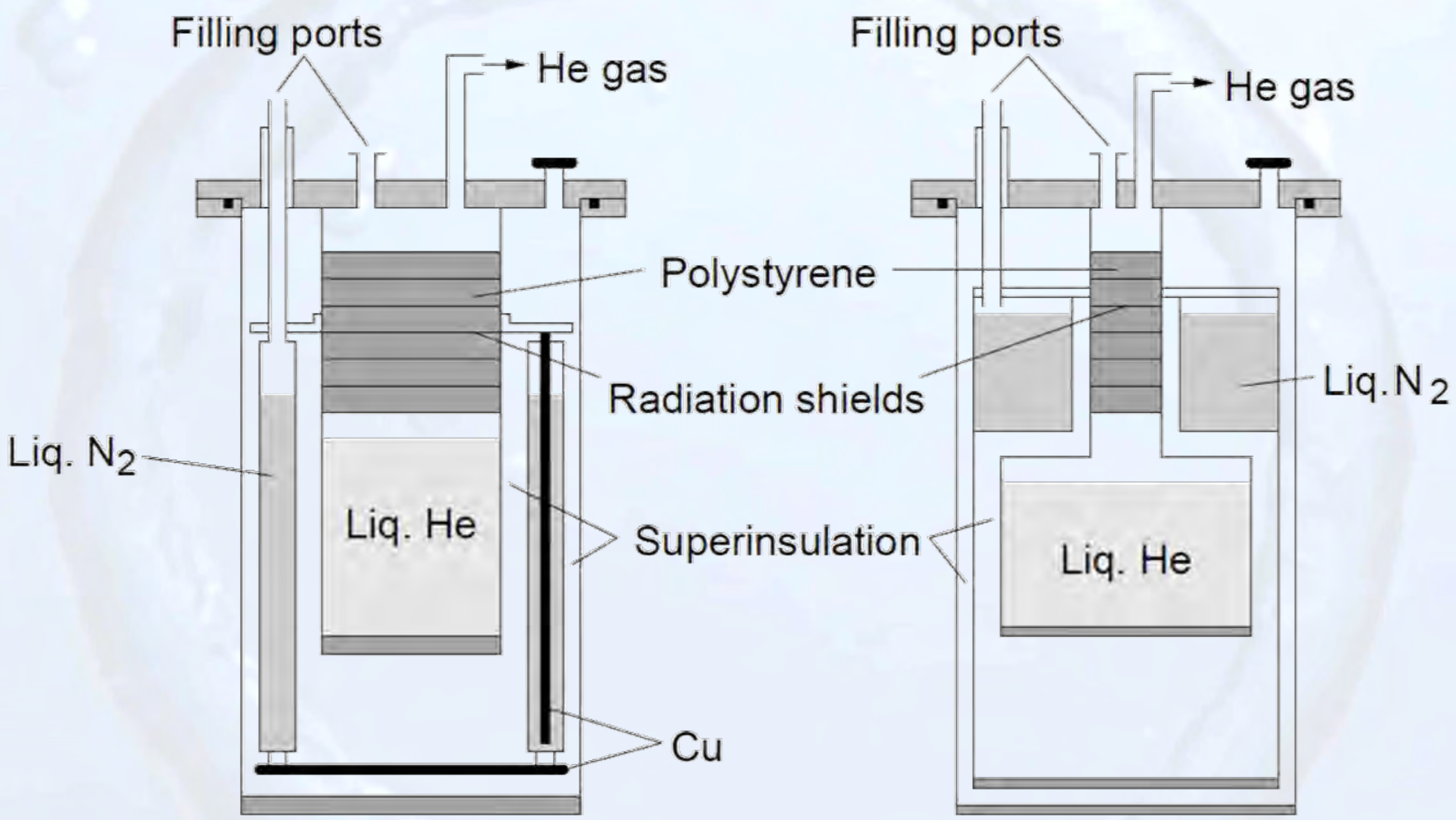

11. Cooling Techniques

helium transport vessel

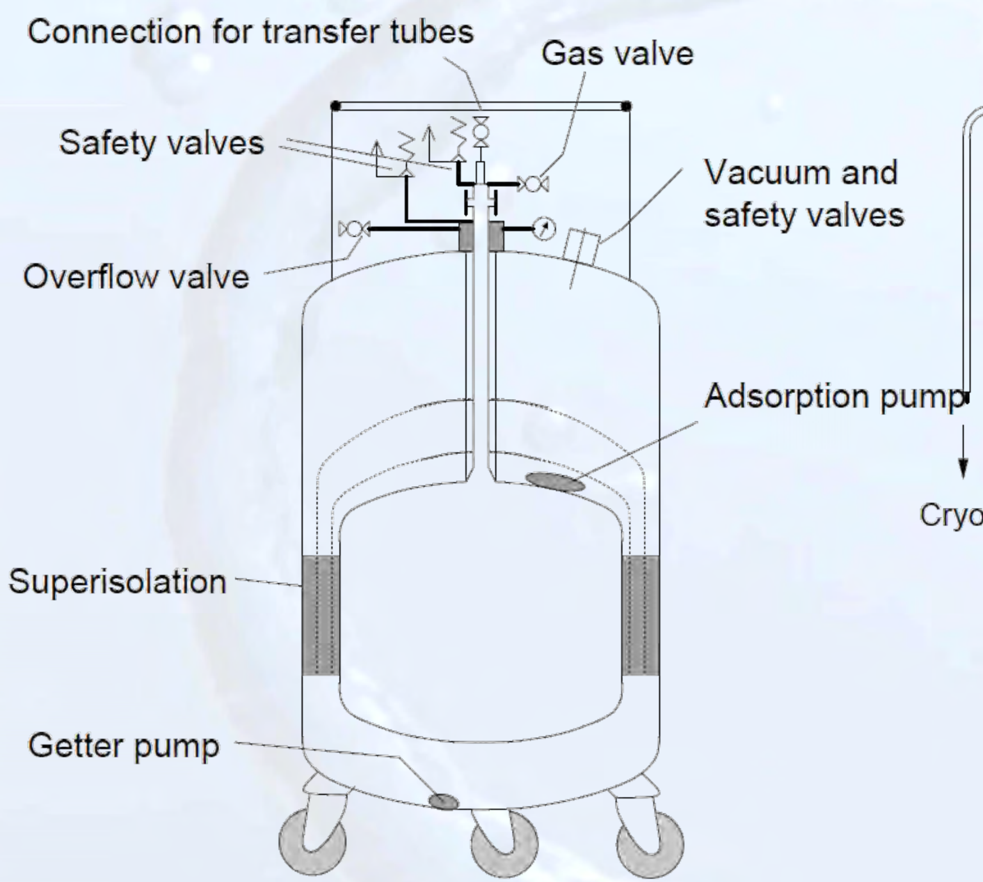

helium transfer tube

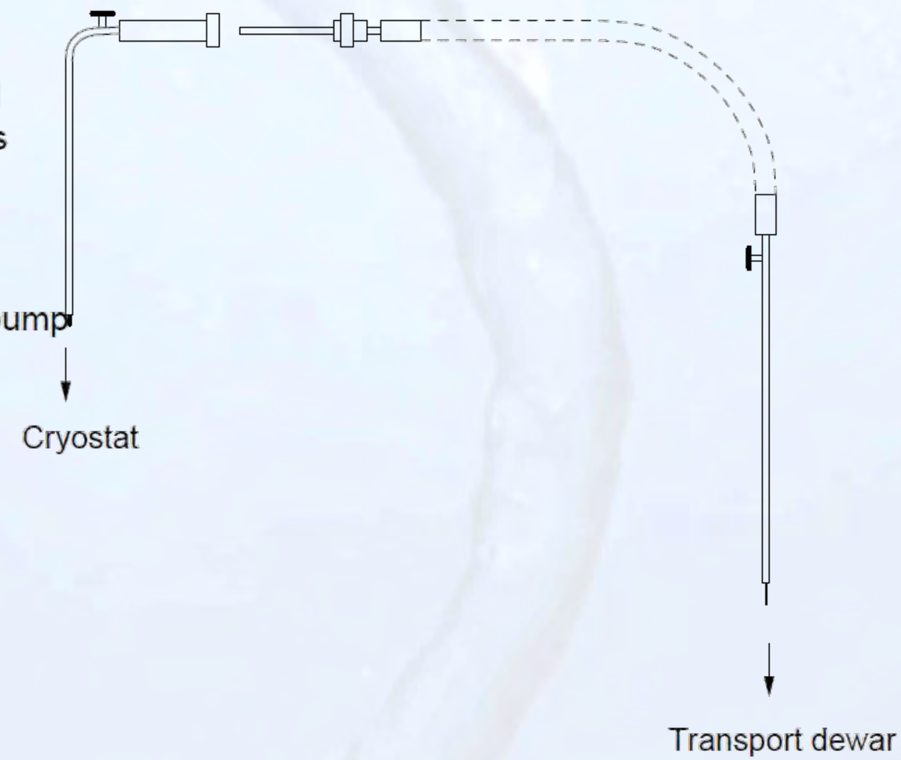

Radiation Shields - Superinsulation

multiple radiation shields → smaller steps → reduction of heat flow

30 to 80 layers of low conductivity
high reflection material → aluminized Mylar

apparent thermal conductivity
$\sim 10^{-4}$ to 10^{-5} W/(m K)